# Measuring Sea Ice Motion

This document describes the derivation of sea ice motion from:

- Passive microwave sensors
- AVHRR
- IABP Buoys
- NCEP/NCAR Winds

The section on Merged Daily Gridded Vectors supports the *Polar Pathfinder Daily 25 km EASE-Grid Sea Ice Motion Vectors* data set, versions 2-4.

# TABLE OF CONTENTS

# 1 ICE MOTION FROM PASSIVE MICROWAVE: SMMR, SSM/I, SSMIS, AND AMSR-E

## 1.1 Methods

The SMMR, SSM/I, SSMIS, and AMSR-E data are re-projected from a polar stereographic projection to a corresponding 25 km EASE-Grid projection. All images are 24-hour composites of all available passes except for SMMR which only has data available every 48 hours. See the "Accuracy" section below for a discussion of the consequences of this. The images cover sea ice areas of both polar regions completely.

The SMMR, SMM/I, SSMIS, and AMSR-E passive microwave instruments have differing channel frequencies, resolutions, and temporal coverage. Detection of ice displacement in passive microwave data were achieved with maximum cross correlation (MCC) techniques described in Emery et al. (1995). The MCC methods were applied to the two SMMR images (37H GHz and 37V GHz channels), the four SSM/I images (37H GHz, 37V GHz, 85H GHz, and 85V GHz channels), the four SSMIS images (37H GHz, 37V GHz, 91H GHz, and 91V GHz channels), and one AMSR-E image (89V). Fowler compared 10 x 10 pixel rectangular subsets of the same spatial locations between two consecutive days and chose the location with the best correlation coefficient. The change in location is considered the ice displacement, which allows ice motion to be calculated. This method applies to each of the channels for each of the four passes.

Because there are two different channels, a higher frequency and lower frequency, used from the SSM/I and SSMIS instruments, the vectors from the two channels are merged together, with vectors available for both frequencies in most cases. The precision of the vectors from the 85 GHz channel is better than that from the 37 GHz channel; however, periods of high water vapor affect 85 GHz more than 37 GHz; so the ability to track ice is reduced. Vectors from 85 GHz are preferable. In cases where 85 GHz and 37 GHz vectors overlap, the 37 GHz vector is removed.

Figure 1 shows a sample of sea ice motion vectors derived from the SSM/I sensor.

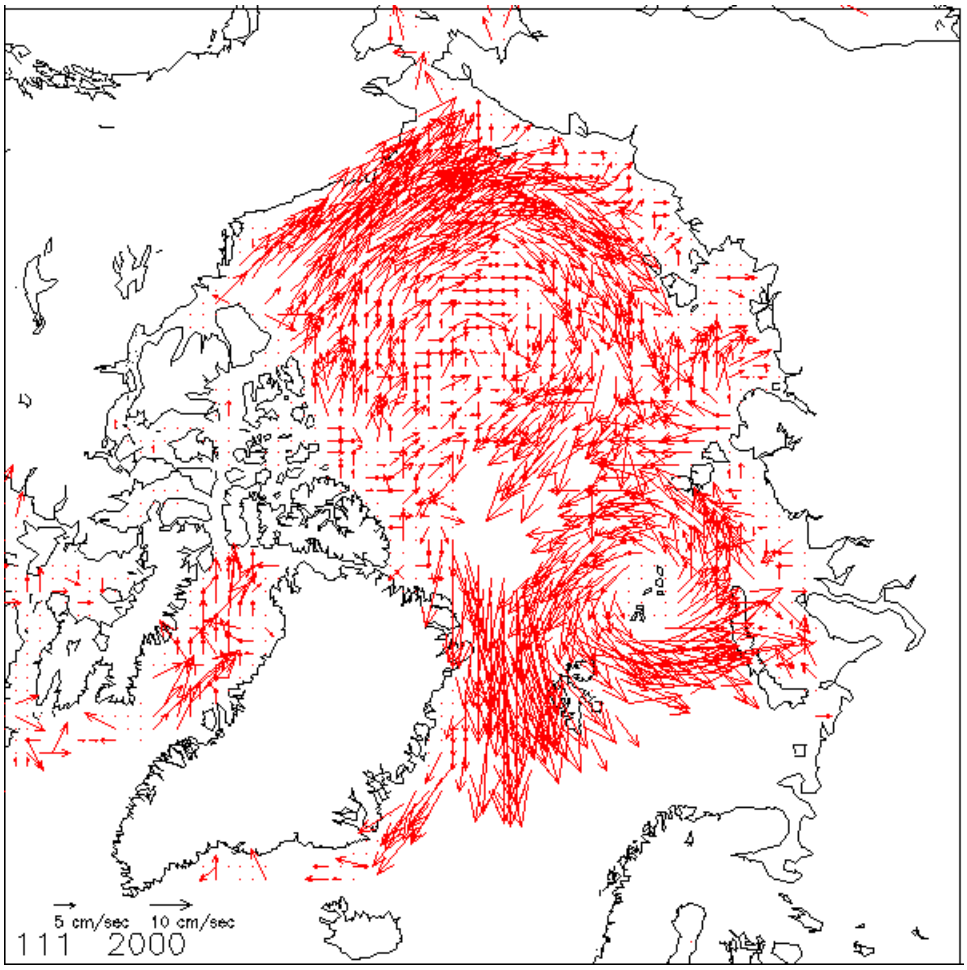

Figure 1. Daily-averaged sea ice motion vectors derived from SSM/I on 20 April 2000

## 1.2 Accuracy

Direct comparisons between the more accurate buoy measurements and vectors derived from passive microwave data are difficult due to time differences. The SMMR data are composites over two days, and the data from the other sensors are composites over a 24-hour period. Each pixel in an image may contain information from more than one orbit, and each pixel represents the composite motion of ice within the pixel area, while buoy motion tracks the drift of a specific ice floe or patch of ice. With these problems in mind, vectors derived from passive microwave imagery were compared with those from buoy data.

For 85 GHz data, there were 74,381 pairs of buoy and SSM/I vectors that were less than 50 km apart. The mean difference in the u component was -0.05 cm/sec with a Root Mean Square (RMS) error of 4.16 cm/sec. The mean difference in the v component was 0.39 cm/sec with an RMS error of 4.23 cm/sec.

For 37 GHz data, the mean difference in the u component was 0.04 cm/sec with a Root Mean Square (RMS) error of 5.05 cm/sec. The mean difference in the v component was 0.74 cm/sec with an RMS error of 5.24 cm/sec.

The pixel resolution of the AMSR-E data is similar to the resolution of the AVHRR data, and the comparison with buoys showed much the same error, with a mean error of 0.19 cm/sec and root-mean-square error of 3.52 cm/sec.

## 1.3 SMMR 48 Hour Temporal Resolution Consequences

The passive microwave motion estimates using SMMR are made using data separated by 48 hours while SSM/I-SSMIS data are 24 hours apart. SMMR data were used from 25 October 1978 through 08 July 1987 when the daily SSM/I data became available.

The daily speeds estimated by SSM/I-SSMIS data appear to be higher than SMMR data, but this is likely primarily explained by the fact that sampling every 24 hours instead of every 48 hours with the same grid spacing yields discrete speed estimates. Two day averages of the net 37 GHz SSM/I ice speeds are comparable to the 48-hour speeds computed from SMMR. However, the motion estimates derived from the horizontal and vertical polarization channels of the higher resolution channel, indicated by a value of 3.0 in the 5th column of the data file, have been found to have larger average speeds than those derived from the 37 GHz channels. This is likely primarily explained by the difference in spatial sampling relative to the time interval.

While these sensor differences affect daily motion estimates in the raw passive microwave fields, average drift aggregated over many motion estimates is largely unbiased. Therefore, these effects are ameliorated in the gridded interpolated files and are minimal in the weekly and monthly average fields.

# 2 ICE MOTION FROM AVHRR

## 2.1 Methods

Data from AVHRR channel 2 (visible band) and channel 4 (infrared) were interpolated to a 5 km resolution EASE-Grid. Channel 4 was used throughout the year, but it is not as useful during melt periods when the ice surface and water are nearly the same temperature. Channel 2 is only useful during sunlit periods in the late spring, summer, and early fall. Figure 2 shows a single orbital swath from AVHRR.

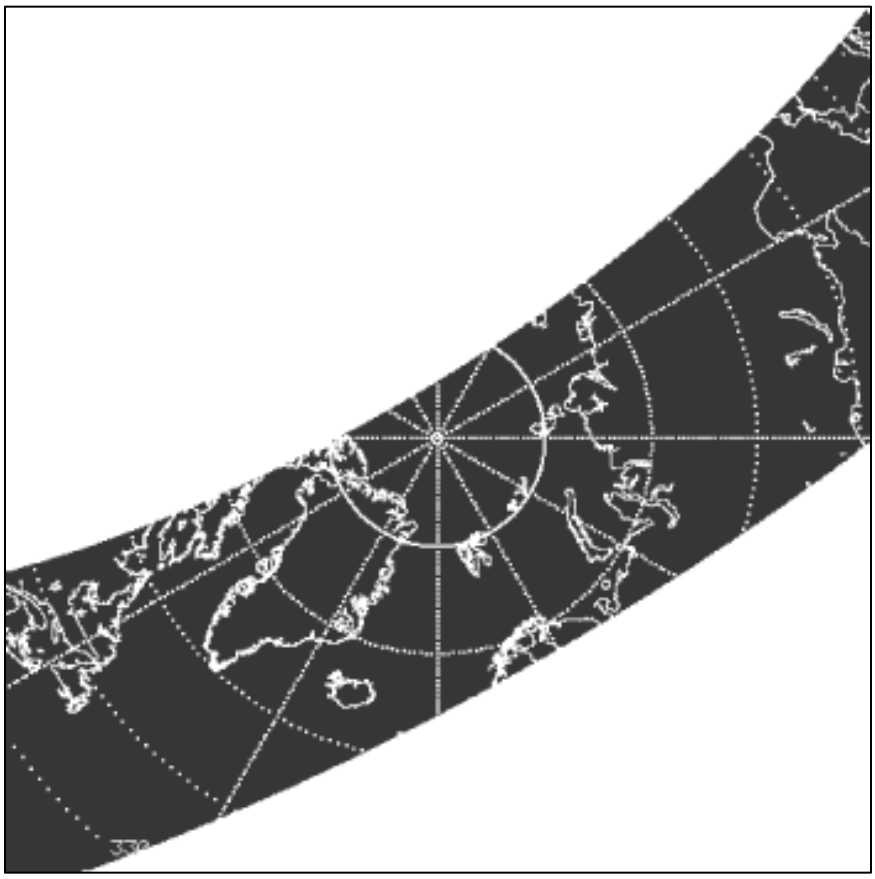

Figure 2. One AVHRR orbital swath

The visible channel is useful during summer melt conditions when microwave and infrared data are unreliable. Thermal imagery is used throughout the year except during the summer melt season when surface ice and water have nearly the same temperature. Ice displacement was derived from four daily satellite passes (0000, 0600, 1200, and 1800 GMT) and matched with the corresponding passes of the next day; therefore, ice velocities from AVHRR data represent average velocities over 24 hours. These four orbits provide full coverage of the ice-covered areas at least once per day, and up to four times near the North Pole, as Figure 3 shows.

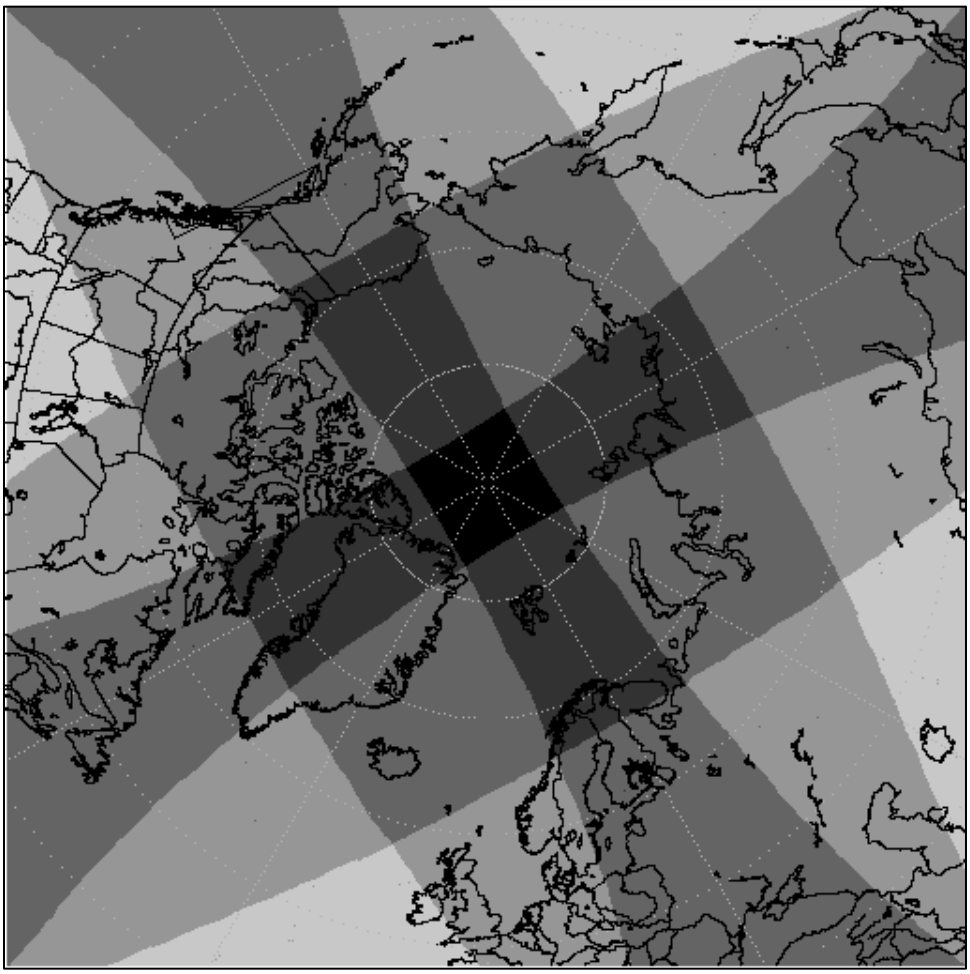

Figure 3. Four daily AVHRR orbital swaths

Calibration is not an issue with ice motion calculations; however, image registration must be optimal, otherwise errors will show a bias in the ice motion. Roll, pitch, and yaw corrections were applied to the navigation stage to minimize error.

Detection of ice displacement in AVHRR imagery was achieved with maximum cross correlation (MCC) techniques described in Emery et al. 1995. Fowler compared 10 x 10 pixel rectangular subsets of the same spatial locations between two consecutive days, and chose the location with the best correlation coefficient. The change in location is considered the ice displacement, which allows ice motion to be calculated. This method applies to each of the channels for each of the four passes.

While AVHRR provides complete satellite coverage of both polar regions, the presence of clouds obscures the surface in both the visible and infrared channels. This is the main limitation with using AVHRR data for calculating ice motion.

An AVHRR Polar Pathfinder ice extent mask was used with the MCC algorithms over ice-covered areas. To detect registration problems, the MCC method was also applied over land. If any

displacements between image pairs occurred over land, Fowler removed this bias from the calculated ice motions. He applied a filter to the calculated vectors to remove "bad" vectors. Assuming the ice moves locally and uniformly, a spatial coherence filter is used to compare each vector with neighboring vectors. If a vector had at least three neighboring vectors that moved in a similar direction to within two pixels, that vector was considered "good."

Cloud contamination is the main reason for eliminating vectors. The MCC method assumes that ice motion of the chosen rectangular area is linear with no distortion or rotation. For most small areas, the non-linearity is small enough to not violate this assumption; however, in areas where ice motion is significantly non-linear, the MCC method cannot effectively track the ice. This is not a significant problem for the 5 km resolution AVHRR data.

All of the vector data for four passes and two channels are averaged together to create a set of daily vectors. Figure 4 contains an example of sea ice motion vectors derived from AVHRR.

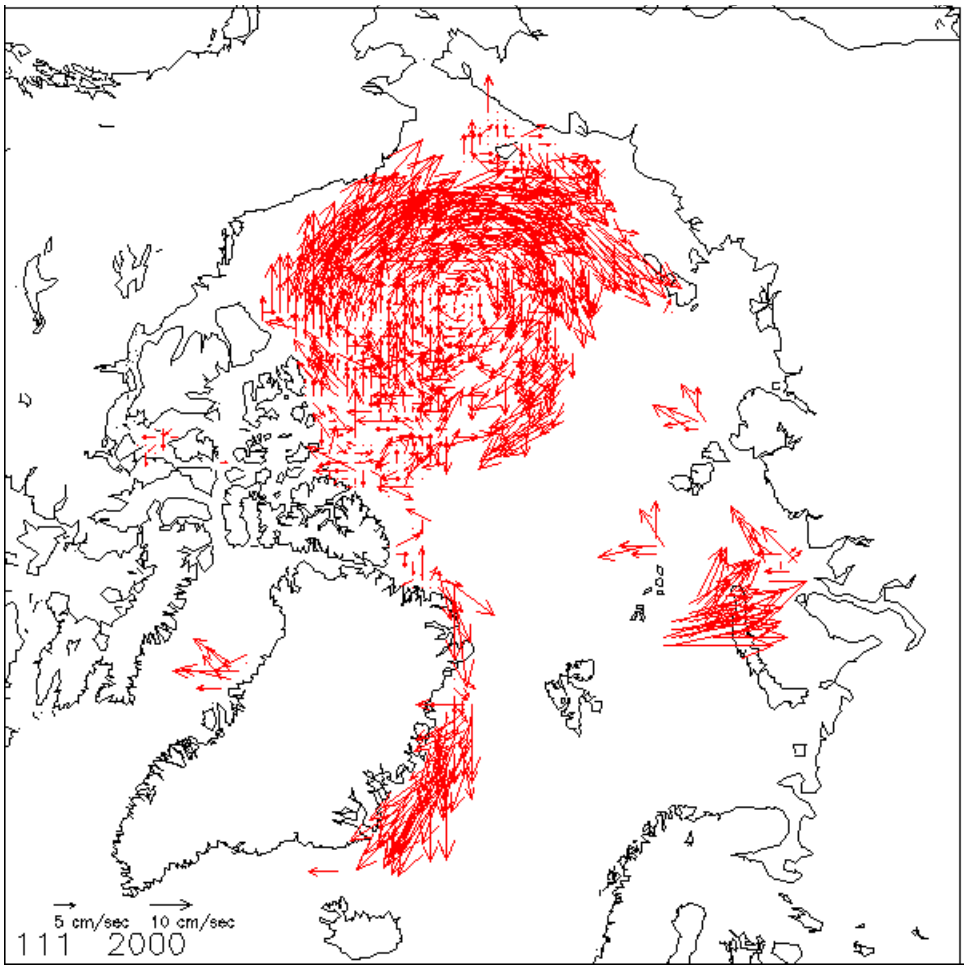


Figure 4. Daily-averaged sea ice motion vectors derived from AVHRR on 20 April 2000

After filtering and merging different passes and channels, the percentage of AVHRR temporal coverage ranges from zero percent to about 40 percent. Figures 5 shows that coverage in the

Canada Basin is nearly 40 percent in the winter but much lower in other areas because of persistent cloud cover.

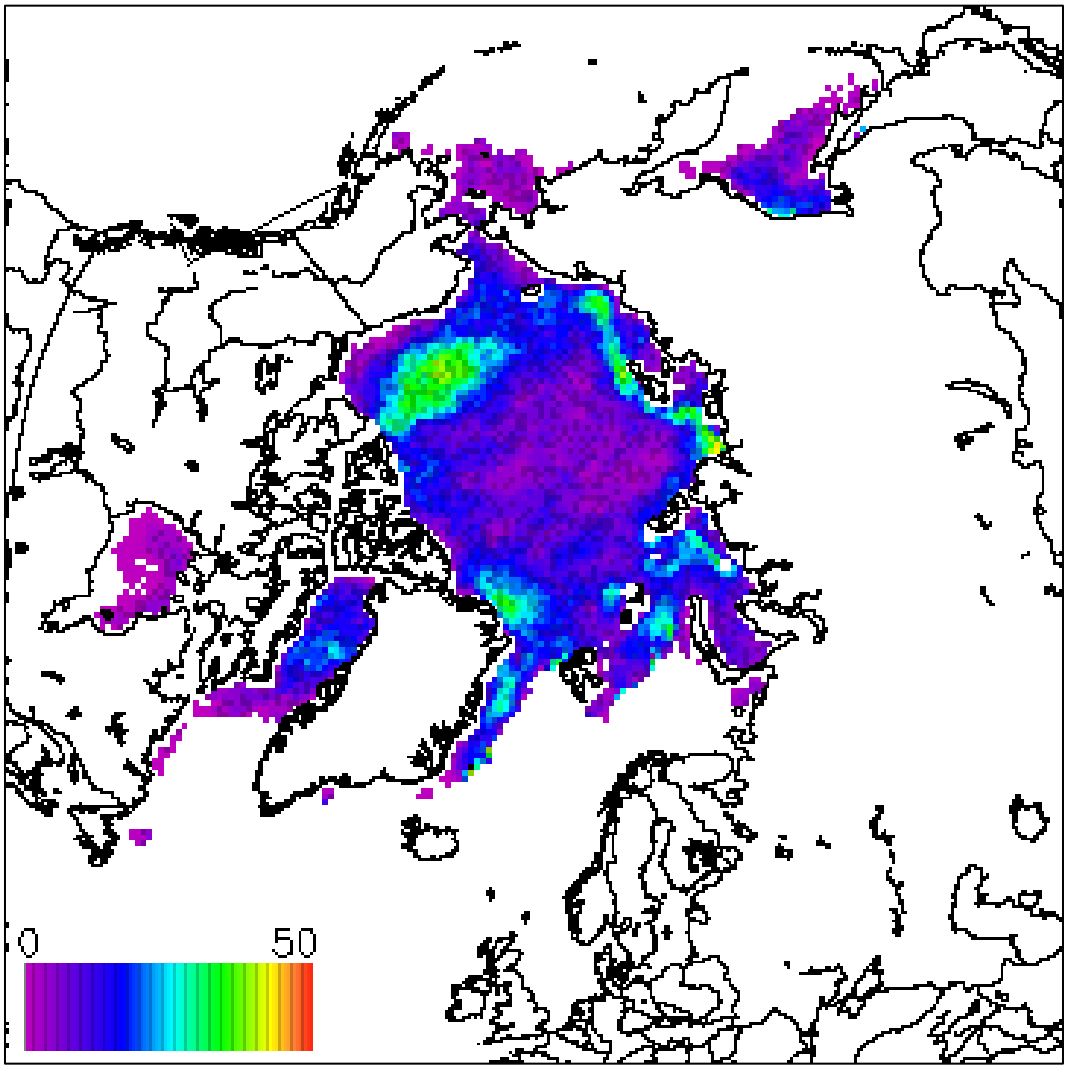


Figure 5. Winter coverage from AVHRR in the Arctic, shown as a percentage of days with a vector

Cloud cover is more prevalent during the summer, resulting in fewer vectors from AVHRR, as shown in Figure 6.

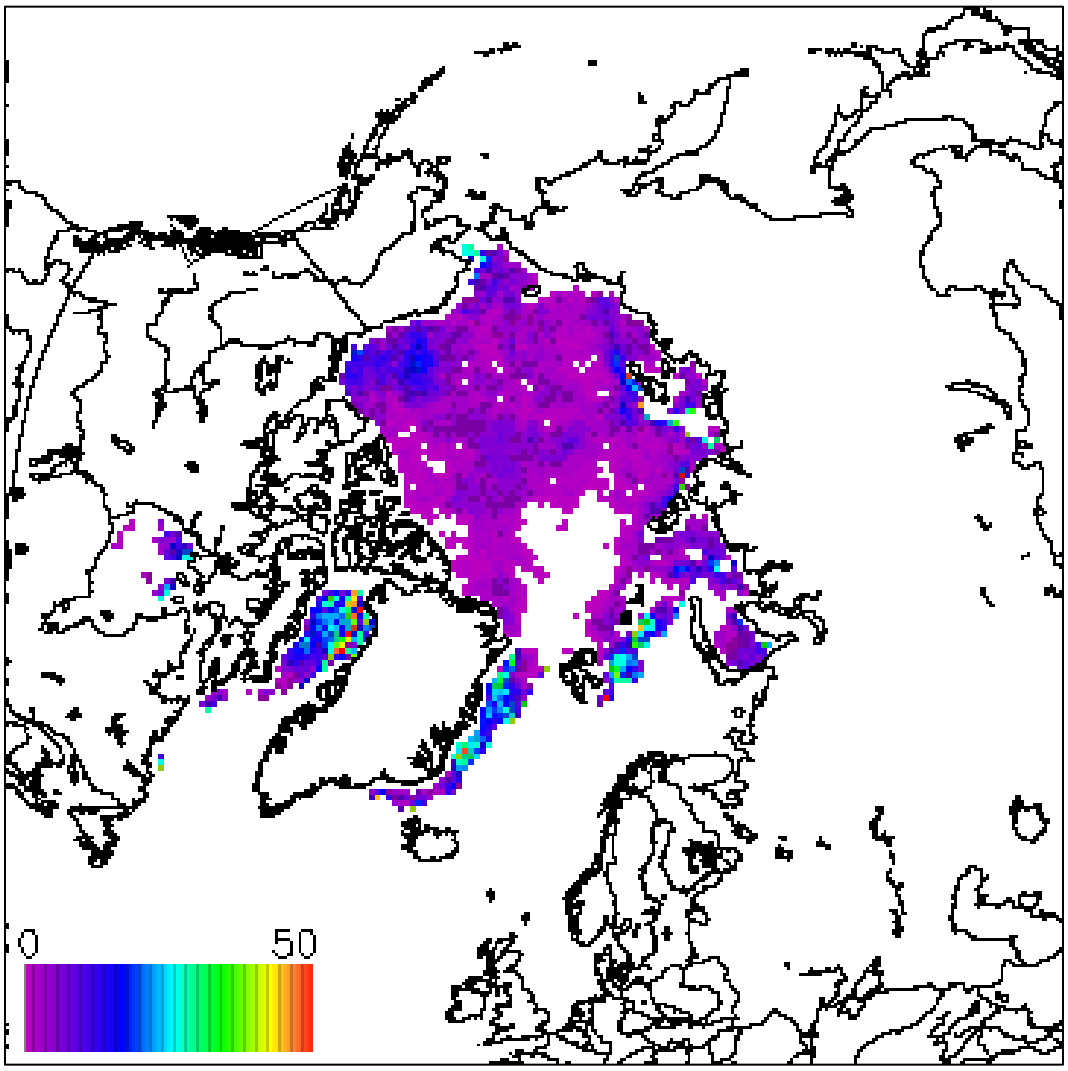

Figure 6. Summer coverage from AVHRR in the Arctic, shown as a percentage of days with a vector

Figure 7 shows that the temporal coverage of vectors derived from AVHRR in the Antarctic region is less than that in the Arctic. Cloud cover is much more persistent and frequent.

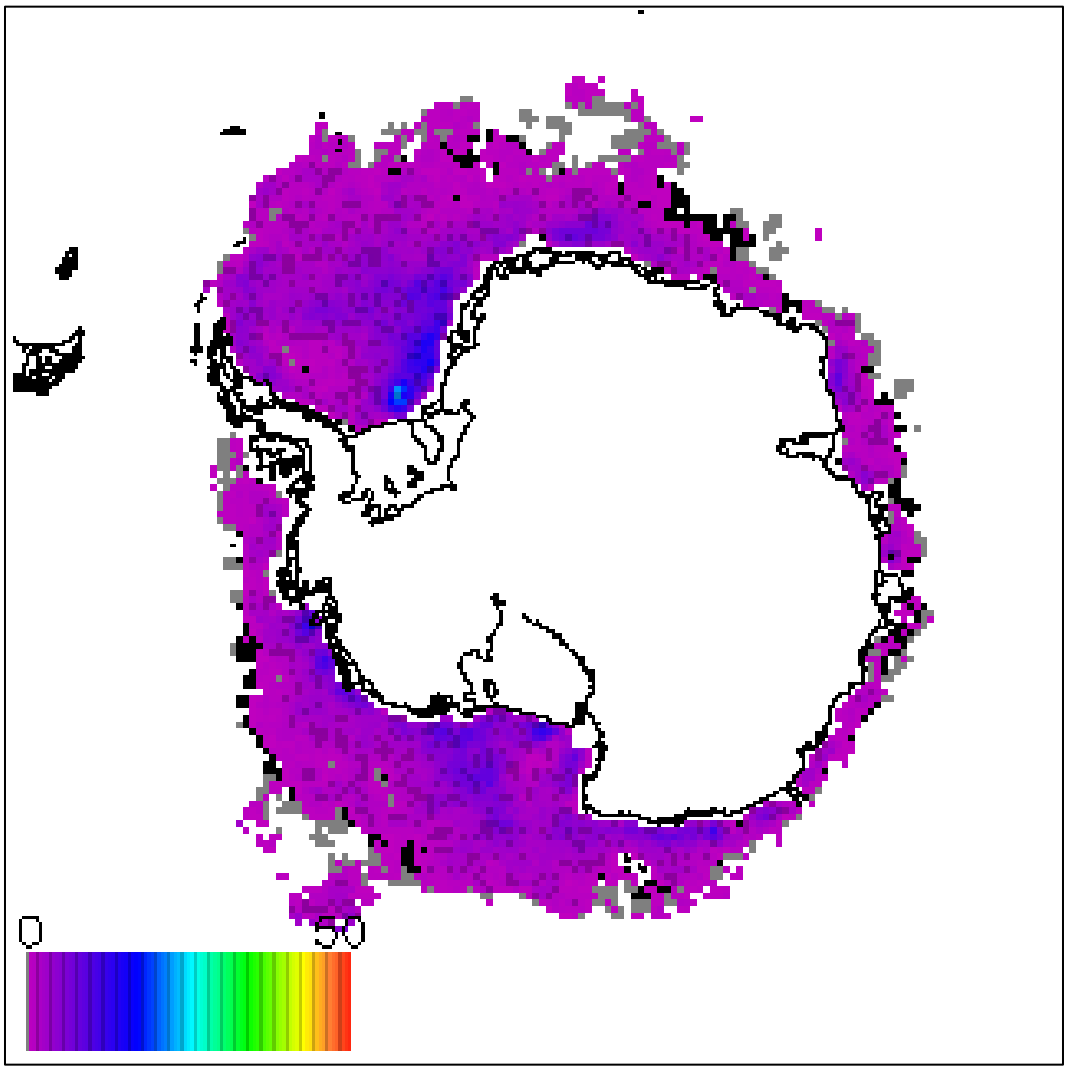

Figure 7. Summer coverage from AVHRR in the Antarctic, shown as a percentage of days with a vector

## 2.2 Accuracy

The MCC method can often detect sub-pixel resolution displacement of ice motion vectors. With satellite imagery, accuracy is between 1/3 and 1/2 pixel displacements. With AVHRR 5 km imagery, ice motion accuracy is about 2 cm/sec. Vectors derived from AVHRR imagery were compared with those from buoy data; 26,820 pairs of AVHRR and buoy vectors were less than 50 km apart. The mean difference in the u component was -0.12 cm/sec with a Root Mean Square (RMS) error of 3.31 cm/sec. The mean difference in the v component was 0.07 cm/sec with an RMS error of 3.29 cm/sec.

# 3 ICE MOTION FROM IABP BUOYS

## 3.1 Methods

Buoy locations from the International Arctic Buoy Programme (IABP) "C" data set were interpolated to six-hour intervals on the 25 km EASE-Grid. Using the 12:00 GMT positions, the distance the buoys traveled in a 24-hour period were calculated. The number of buoys and their locations varies from year to year, but the maximum number is about 30 buoys. Usually these buoys are widely spaced; very few are placed in the Eastern Arctic.

Figure 8 shows a sample of sea ice motion vectors derived from buoys.

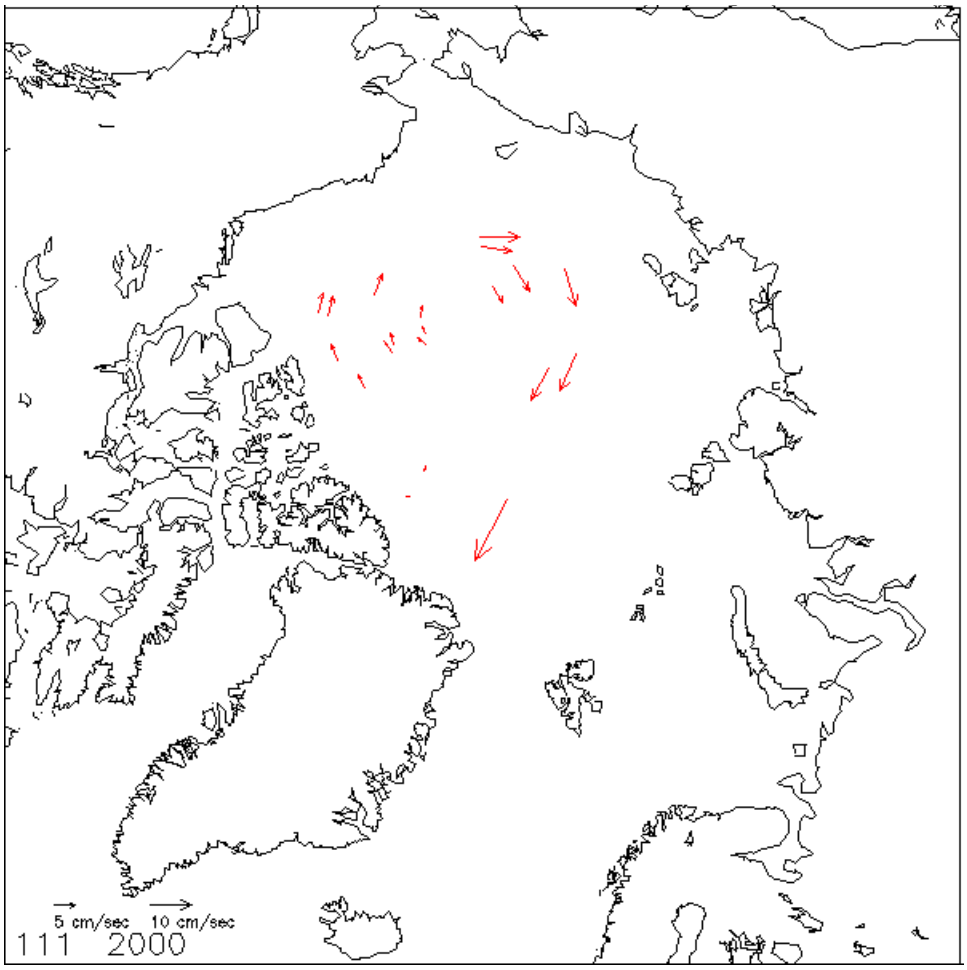


Figure 8. Daily-averaged sea ice motion vectors derived from buoys on 20 April 2000

## 3.2 Accuracy

It is difficult to assign an error value to a buoy velocity. The position accuracy of the buoys is about 0.5 km. The locations are interpolated to the 6-hour interval times. The accuracy is then dependent

upon the initial position error and the interpolation error. It could be assumed that the overall error would be less than 1 cm/sec for the average velocity over 24-hours.

# 4 ICE MOTION FROM NCEP/NCAR WINDS

## 4.1 Methods

Due to melting ice during the summer months, passive microwave data is mostly unusable for determining ice motion; and because cloud cover obscures ice detection in AVHRR's infrared and visible wavelengths, far fewer vectors are generated. Only the relatively few buoy vectors are available all year, and these are mostly located on multi-year ice. Since there is much more first year ice covering the Arctic basin in the last decade, ice motion vectors derived from NCEP/NCAR wind reanalysis fields have been added. The NCEP/NCAR estimates are interpolated to the 25 km EASE-Grid projection. Thorndike and Colony (1982) found that, during summer conditions, the ice moves approximately one percent the speed of the wind and has a turning angle of about 20 degrees from the wind. This general rule was applied to the NCEP/NCAR winds. Adding these vectors deviates from only using vectors derived from remote sensing instruments, but they help to provide information to areas with little coverage.

Figure 9 shows a sample of sea ice motion vectors derived from NCEP/NCAR Winds.

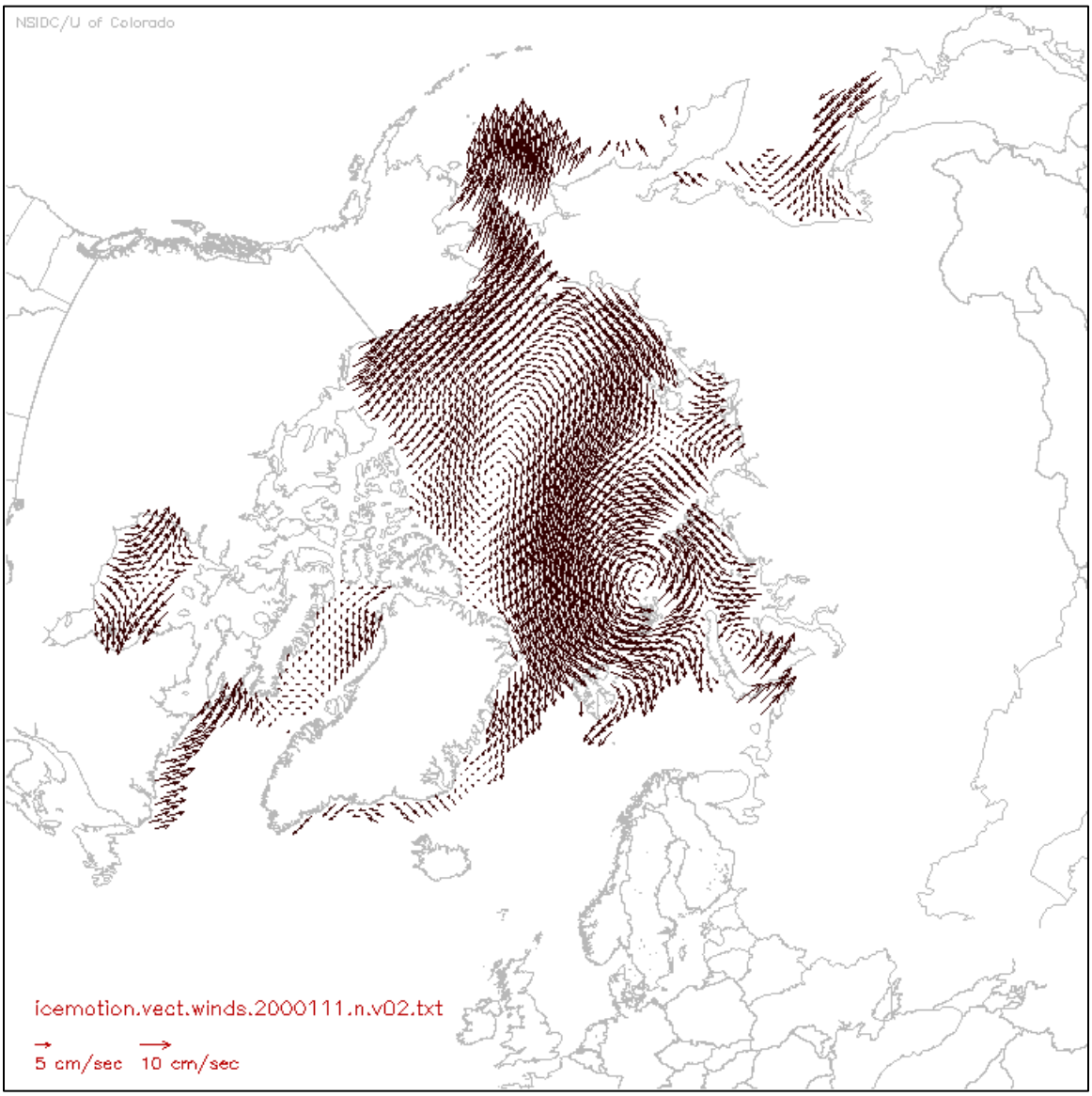


Figure 9. Daily-averaged sea ice motion vectors derived from NCEP/NCAR Winds

## 4.2 Accuracy

The accuracy of the ice vectors from wind fields will not be as good as from other sources. First, the wind fields are from atmospheric models, not directly from satellite or buoy observations. Second, the relationships between winds and ice motion are just general rules. Comparisons with buoys show mean differences of 1.2 cm/sec and Root Mean Square (RMS) error of 6.1 cm/sec.

# 5 MERGED DAILY GRIDDED VECTORS

## 5.1 Methods

Optimal interpolation was used to create daily gridded ice motion fields from SMMR, SSM/I-SSMIS, AMSR-E, AVHRR, IABP buoy data, and NCEP/NCAR wind data. A cokriging estimation method described by Isaaks and Srivastava (1989) was employed for the interpolation. This method utilizes the cross-correlation between several variables—in this case, the vectors derived from SMMR, SSM/I-SSMIS,AMSR-E, AVHRR, IABP buoy data, and NCEP/NCAR winds—to minimize the estimation error variance. See Figure 10 for more details.

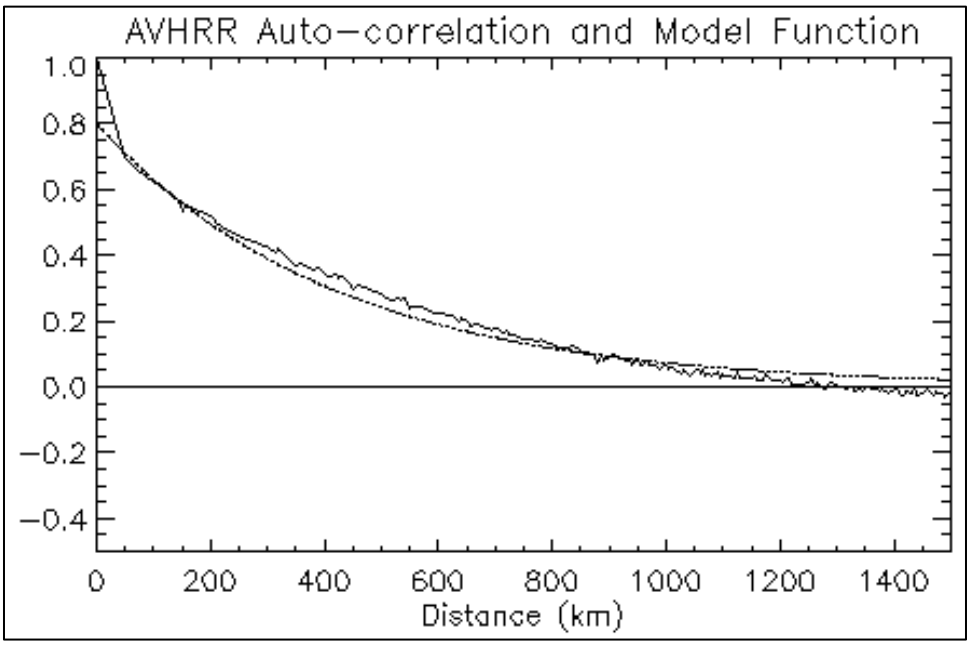


Figure 10. Example of autocorrelation (jagged line) for the u component of the vectors derived from AVHRR

### 5.1.1 Autocorrelation

The plot shows discontinuity near 50 km distance. If discontinuity is ignored, the autocorrelation line would cross the zero-distance line at about 0.8. This value, which is related to measurement error, is often referred to as the "nugget effect" in geostatistics. The shape of the curve is similar for both u and v vector components and for all of the auto-correlation and cross-correlation functions among all of the data sets. The major difference is the starting point at zero km distance. The autocorrelations for the ice motions for AMSR-E were very similar to AVHRR, and the vectors from the wind data were very close to the 37 GHz vectors. See Table 1 for more details.

Table 1. Starting points for each of the auto- and cross-correlations

| | BUOY | AVHRR/AMSR-E | SSM/I-SSMIS 85 GHz | SMMR or SSM/I-SSMIS 37 GHz/Winds |
|---|---|---|---|---|
| **BUOY** | .95 | .70 | .70 | .40 |
| **AVHRR/AMSR-E** | | .85 | .65 | .30 |
| **SSM/I-SSMIS 85 GHz** | | | .80 | .40 |
| **SMMR or SSM/I-SSMIS 37 GHz/Winds** | | | | .45 |

A simple exponential function was used to model the correlation (dotted line) in the above figure. This function provided the best model to approximate the vector data. Cross-correlations between the u and v components were performed over the entire Arctic and Antarctic regions, and it was found that they were nearly independent. The u and v components were thus treated independently and were interpolated separately for simplicity. Using the modeled correlation functions, vectors for each ice-covered area on the 25 km EASE-Grid were interpolated. See Figure 11 for an example.


Figure 11. Vector plot for 20 April 2000, where every fourth vector is plotted

### 5.1.2 Sample daily-averaged vector plot

The number of vectors from the buoy, passive microwave, and AVHRR data varies. A plot of monthly average percent coverage of ice-covered areas shows that summer weather conditions affect the ability of satellites to track ice. Figure 12 shows the percentage of sea ice grid cells that contain vectors.

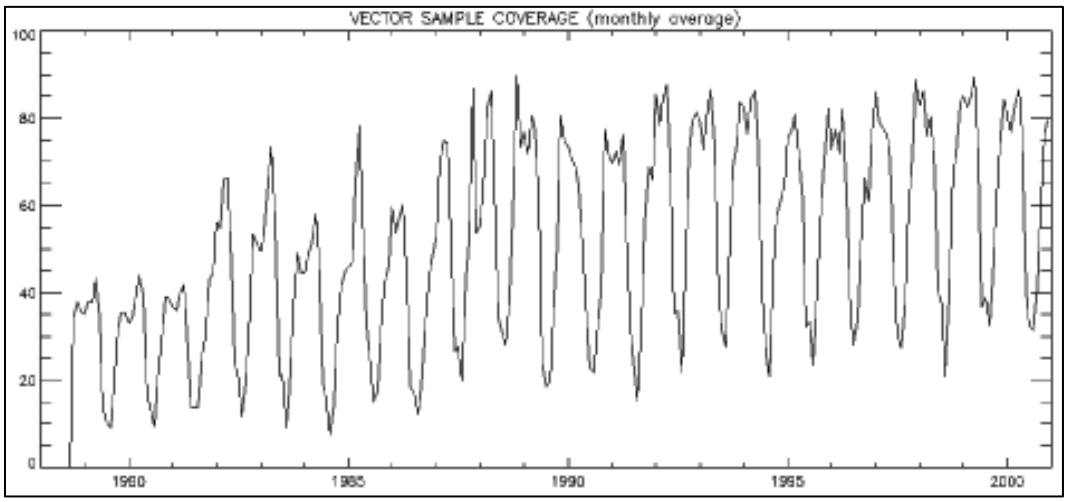


Figure 12. Percent coverage of sea ice grid cells

Figure 13 shows the average number of vectors available from each source.

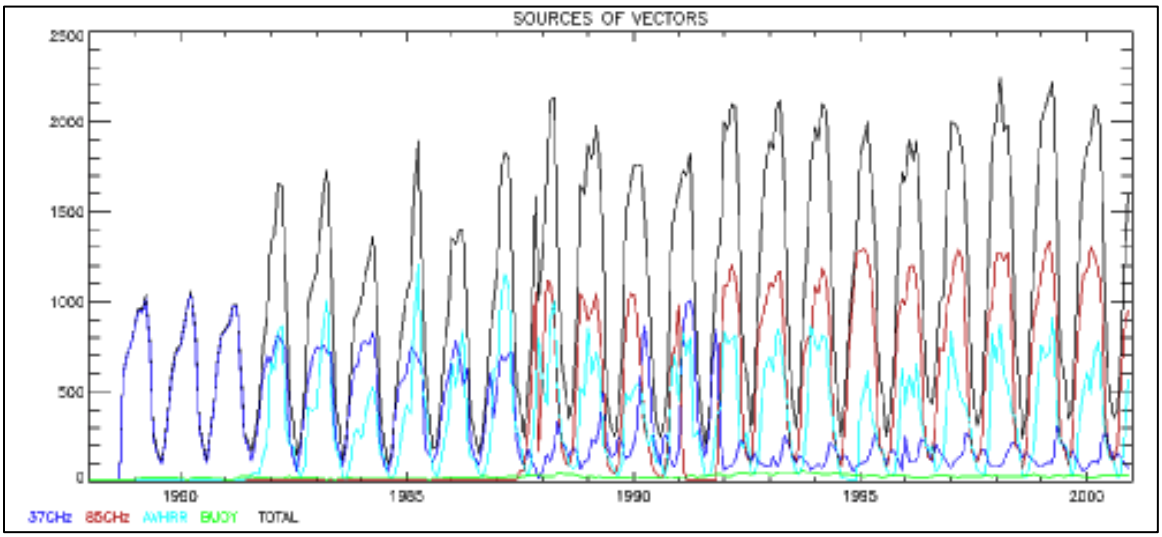


Figure 13. Number of vectors from each source

Similarly, Figure 14 shows the percentage of available vectors from each source.

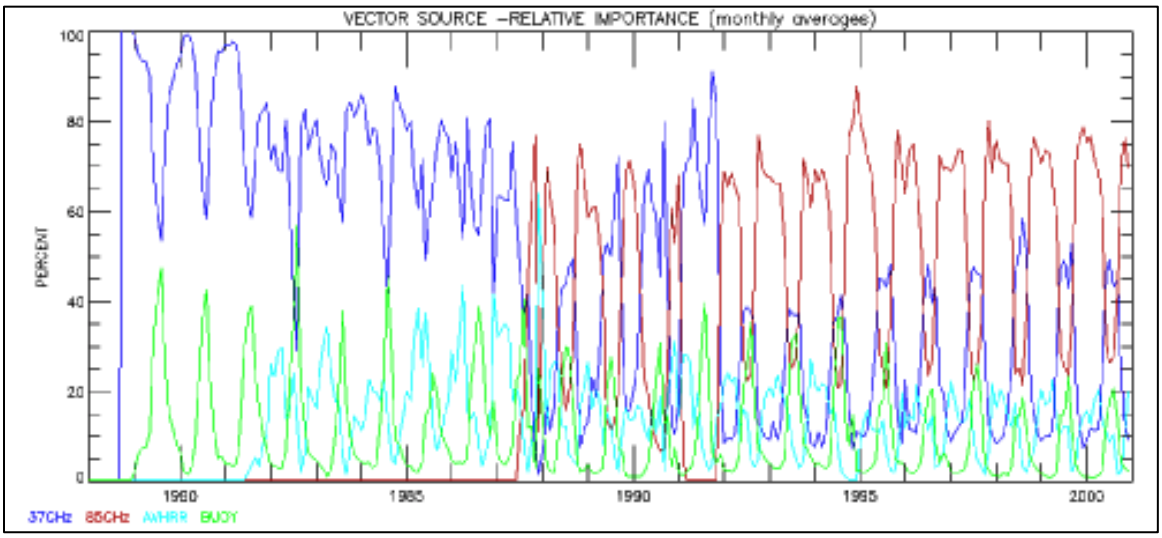


Figure 14. Percentage of vectors from each source

Note that the vectors from the 85 GHz channels began in 1987 with the launch of the SSM/I instrument.

## 5.2 Accuracy

Several years of vectors were interpolated to the same grid for comparison, but without using the buoy data. The mean difference between the interpolated u components and the buoy vectors was 0.1 cm/sec with a Root Mean Square (RMS) error of 3.36 cm/sec. For the v component, the mean was 0.4 cm/sec with an RMS error of 3.40 cm/sec.

## 5.3 Limitations

Gridded vector fields are not the optimal data set for everyone. They are best used for evaluating climatological patterns and changes in sea ice motion over the last 25 years. Various assumptions were factored into the production of gridded vector fields. For optimal interpolation, the data should be stationary, homogenous, and isotropic. Sea ice does not have these characteristics. Changes in ice concentration and thickness may negate the assumptions. In an ideal case, two-dimensional correlation functions are found at every grid location on each day to help alleviate some of these problems.

Another limitation of the data is cloud cover, which can affect a satellite's ability to discern sea ice, and thus, the number and location of available vectors on each day.

Data users should use the summer vector plots with caution due to the low number of vectors resulting from surface melt and increased cloud cover in the summer. As individual summer daily plots contain significant noise, weekly- and monthly-mean plots are more reliable.

# 6 REFERENCES

Emery, W., C. Fowler, and J. Maslanik. (1995). Satellite Remote Sensing of Ice Motion. In M. Ikeda & F. W. Dobson (Eds.). *Oceanographic Applications of Remote Sensing.* Boca Raton: CRC Press.

Thorndike, A. S., & Colony, R. (1982). Sea ice motion in response to geostrophic winds. *Journal of Geophysical Research*, *87*(C8), 5845. https://doi.org/10.1029/JC087iC08p05845